Hindawi Publishing Corporation
International Journal of Photoenergy
Volume 2006, Article ID 90809, Pages 1–6
DOI 10.1155/IJP/2006/90809

Nanocrystalline TiO_2 with Enhanced Photoinduced Charge Separation as Catalyst for the Phenol Degradation

Carmen Canevali,[1] Franca Morazzoni,[1] Roberto Scotti,[1] Ignazio Renato Bellobono,[2] Marco Giusti,[1] Marco Sommariva,[1] Massimiliano D'Arienzo,[1] Andrea Testino,[1] Anna Musinu,[3] and Carla Cannas[3]

[1] *Department of Materials Science, University of Milano-Bicocca, Via R.Cozzi 53, 20125 Milan, Italy*
[2] *Environmental Research Centre, University of Milan, Via C. Golgi 19, 20133 Milan, Italy*
[3] *Dipartimento di Scienze Chimiche, Università di Cagliari, INSTM, SS554 Bivio per Sestu, 09042 Monserrato (CA), Italy*

Received 15 February 2006; Accepted 23 March 2006

Nanocrystalline TiO_2 catalysts based on pure rutile (R100) and a 30% of anatase and 70% of rutile (R70) were synthesized by the sol-gel method, using Pluronic PE 6400 as templating agent. Catalysts were characterized in terms of structural and morphological properties; moreover, the formation of paramagnetic charge carriers under UV irradiation was studied and related to the activity of TiO_2 in the photoinduced degradation of phenol. With respect to Degussa P25, the two sol-gel catalysts show lower surface area and a wider pore size distribution. The EPR spectra recorded under UV irradiation show enhanced charge separation in the sol-gel samples, with the O^- species in higher amount than in Degussa P25. This result is in agreement with the high catalytic activity of R100 sample in the photoinduced degradation of phenol, very similar to that displayed by Degussa P25 and higher than that of R70 sample.

1. INTRODUCTION

Titanium dioxide is a very active photocatalyst stable in most chemical environments, inexpensive, and of low biological toxicity [1]. These properties justify its use in several industrial applications, including water remediation through the degradation of organic contaminants [2, 3], removal of gaseous organic and inorganic pollutant [4, 5], odor control [6, 7], and protective coatings [8]; moreover, they have led to the development of commercial products such as self-cleaning materials [9], air cleaning ceramic tiles [10], and self-disinfecting medical products [11].

Many TiO_2 formulations have been developed as catalysts, exhibiting different photoefficiencies. In general, anatase has long been considered the most photochemically active phase of TiO_2, probably because of a higher surface adsorptive capacity towards many organic compounds [12], while the rutile phase is generally less active because of higher rates of recombination of the photogenerated charge carriers [13]. On the other hand, mixed-phase materials, as the commercial Degussa P25, show higher photocatalytic activity than pure phases [14]. Degussa P25 consists of 80% anatase and 20% rutile [15] and is normally used as a reference material for the catalytic activity of TiO_2.

The charge carriers photogenerated in TiO_2 by UV irradiation are electrons in the conduction band (CB) and holes in the valence band (VB) [16] (reaction 1). Then, holes are trapped at bulk or surface O^{2-} ions giving paramagnetic O^- species [17] (reaction 2); while electrons are trapped on Ti^{4+} ions located at the bulk, at the surface [16, 18] and, in mixed-phase systems, at the anatase-rutile interface, giving EPR active Ti^{3+} species [19] (reaction 3):

$$TiO_2 + h\nu \longrightarrow e^-_{CB} + h^+_{VB}, \quad (1)$$

$$O^{2-} + h^+_{VB} \longrightarrow O^-, \quad (2)$$

$$Ti^{4+} + e^-_{CB} \longrightarrow Ti^{3+}. \quad (3)$$

According to reactions 1–3, the paramagnetic species Ti^{3+} and O^- may be considered as probes of the photogenerated electrons and holes, respectively, and can be revealed by electron paramagnetic resonance (EPR) spectroscopy. In particular, EPR was used to study the charge transfer processes which occur within Degussa P25 TiO_2 [19–21]. For this commercial mixed-phase catalyst, it was suggested that its high photoactivity is due to: (i) the lower band gap energy of rutile, which extends the useful range of photoactivity into the visible region, and (ii) a slower charge recombination due to an efficient electron transfer from rutile to anatase, which

is favored by an intimate contact between anatase and rutile particles [20]. In particular, the EPR-active electron trapping sites at the interface between rutile and anatase were proposed as catalytic hot spots for the mixed-phase TiO_2 catalyst [19]. In spite of the studies on Degussa P25 and on pure phases [22, 23], the design of new catalysts with improved efficiency needs a much more wide correlation between photocatalytic properties and charge carriers. With this aim, in the present paper, pure rutile and a mixed-phase TiO_2 were synthesized by template-assisted sol-gel method. This generally allows a good control in terms of composition and morphology in the nanoscale particle size range. The paramagnetic species formed on these catalysts under UV irradiation and their activity in the photoinduced degradation of phenol were studied and compared with those of the commercial product.

2. MATERIALS AND METHODS

2.1. Reagents

Titanium(IV) chloride ($TiCl_4$, ≥ 99.9%), ethanol (≥ 99.9%), HCl (37%), phenol (≥ 99%), and H_2O_2 (35%) were from Aldrich and used as supplied. Triblock copolymer $EO_{13}-PO_{30}-EO_{13}$ (Pluronic PE 6400, EO = $-CH_2CH_2O-$, PO = $-CH_2(CH_3)CHO-$) was a gift from BASF. Degussa P25 was purchased from Degussa Corporation. All chemicals were used as received. Mill-Q water was used. Pure nitrogen and oxygen were supplied by Sapio.

2.2. Preparation of the catalysts

Following the synthetic procedure described in the literature [24, 25], pure rutile and a mixed-phase TiO_2 photocatalysts were synthesized by a sol-gel process using a triblock copolymer as templating agent.

In a typical synthesis, 1.5 g of the triblock copolymer Pluronic PE 6400 were dissolved in ethanol (19 ml) under magnetic stirring. In order to obtain pure rutile phase (sample R100), HCl 37% (0.01 mol) was added to the polymer solution. Then, $TiCl_4$ (0.01 mol) was added dropwise under N_2 atmosphere within 30 minutes. The sol-gel transition occurred after 6 days in air at room temperature. Care was taken in order that all samples had the same area of exposed surface (24 cm^2). Aging of gels went on for 15 days in air at room temperature; the obtained xerogels were finally calcined in O_2 at 653 K for an overall time longer than the thermal treatment reported in the literature [24, 25], typically 15 hours, until the triblock copolymer was removed and a white TiO_2 powder was obtained.

2.3. Characterization of the catalysts

The X-ray diffraction (XRD) patterns were obtained on a Bruker D8 Advance diffractometer using Cu Kα radiation. The phase content was determined by the Rietveld method.

Nitrogen adsorption-desorption measurements were carried out on a Sorptomatic 1990 System (Fisons Instruments) to determine the specific surface area (SSA) and the total pore volume (V_P) by the BET method [26] and to estimate the pore size distribution using Barrett-Joyner-Halenda (BJH) procedures. Before measurement, samples were evacuated at 473 K for 12 hours.

Transmission electron microscopy (TEM) dark field (DF) images were obtained with a JEOL 200 CX microscope operating at 200 kV. For the analysis, powders were dispersed in *n*-octane by sonication and a drop of the dispersion deposited on a carbon film supported by a copper grid. Particle size was obtained by measuring the diameter D_i of the particles for a number of particles close to 500 from different parts of the grid for each sample. Average particle size was calculated with a log normal distribution.

High-resolution transmission electron microscopy images were obtained with a JEM 2010 UHR, equipped with a Gatan imaging filter (GIF) and a 794 slow scan CCD camera.

EPR spectra were recorded at 10 K on a Bruker EMX spectrometer working at the X-band frequency, equipped with an Oxford cryostat operating in the range of temperature 4–298 K. Spectra were recorded on powder samples in helium atmosphere, both before and after 30 minutes of irradiation within the EPR cavity. For irradiation, an UV 500 W Hg lamp (Jelosil, Italy) was used, equipped with the output radiation focalized on sample in the EPR cavity. The *g* values were determined by standardization with α,α'-diphenyl-β-picryl hydrazyl (DPPH). The intensity of the EPR signal, expressed in arbitrary units, was calculated with a ±10% accuracy by double integration of the resonance lines. Care was taken in order that the sensitive part of the EPR cavity (1 cm length) was always filled.

2.4. Photoinduced degradation of phenol

Reactions were carried out in a 400 ml pyrex discontinuous batch reactor with an external coil jacket and equipped with a UV 125 W Hg high pressure lamp placed in a coaxial quartz cylinder. No optical filter was adopted. The reactor was externally enveloped in an aluminum foil.

Titanium dioxide (100 mg) was suspended by sonication in 400 ml of an aqueous solution containing phenol at the concentration of 121 mg/l (93 mg/l as C). Then, stoichiometric H_2O_2 35% (molar ratio phenol: H_2O_2 = 14 : 1) was added, the suspension was stirred in the dark for 30 minutes, then the UV source was turned on. The temperature was kept at 298 K. For the monitoring of the photoinduced degradation of phenol, an aliquot of the reaction solution (6 ml) was drawn out at regular time intervals, centrifuged in order to separate TiO_2 powder, then the clear solution was analyzed by means of the total organic carbon (TOC) analyzer TOC-*V* CSH (Shimadzu). The overall precision of the analysis was ±8%.

Control experiments were carried out in the absence of TiO_2 (blank) and with Degussa P25. The experimental points were fitted with the integral of a Gaussian curve. In order to compare the kinetics of the different samples, the maximum slope point, which corresponds to the maximum degradation speed, $(dC/dt)_{max}$, and the correspondent time value, $t_{1/2}$, were selected as characteristic parameters.

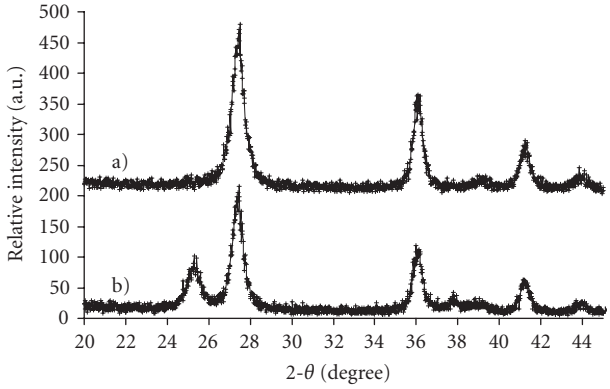

Figure 1: Wide angle XRD patterns of TiO_2 after calcination at 653 K: (a) pure rutile (sample R100), (b) mixed-phase TiO_2 containing 30% anatase and 70% rutile (sample R70).

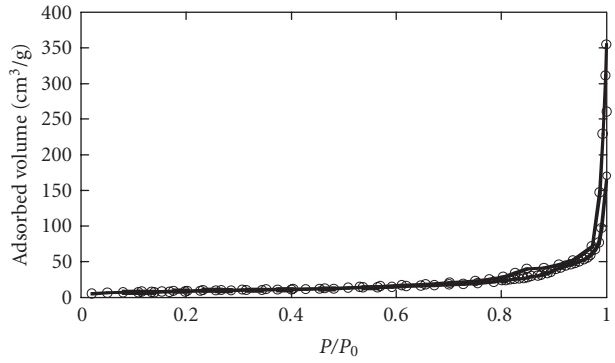

Figure 2: N_2-physisorption curves recorded at 77 K for the R100 TiO_2 catalyst.

3. RESULTS AND DISCUSSION

3.1. Structural and morphological characterization of the catalysts

The wide angle XRD patterns of the sol-gel TiO_2 catalysts after calcinations at 653 K are shown in Figure 1. The diffraction peaks were indexed as pure rutile TiO_2, sample R100 in Figure 1 (JCPDS, no. 21–1276) and bicrystalline anatase and rutile (for anatase, JCPDS, no. 21–1272). For this latter sample, the phase content was calculated by the Rietveld method and resulted to be 30% for anatase and 70% for rutile (sample R70 in Figure 1).

The nitrogen adsorption-desorption curves in Figures 2 and 3 can be assigned to type II isotherms (IUPAC classification) with a small hysteresis loop. The BET surface area values of 31 and 44 m^2/g and the pore volume of 0.15 and 0.23 cm^3/g were obtained for R100 and R70 samples, respectively. The surface area values are slightly lower than the value reported in the literature for Degussa P25 (51 m^2/g) [15], while the total pore volumes were very similar to that of the commercial product (0.15 cm^3/g) [15] (Table 1). However, while Degussa P25 shows a small characteristic pore distribution in the range 30–40 nm, on both sol-gel samples a pore size distribution rather heterogeneous with pore sizes ranging from 2 to 100 nm was observed. This result is probably due to the prolonged calcination at 653 K, which was necessary to remove the triblock copolymer Pluronic PE 6400 and obtain a white TiO_2 powder.

The phase content, specific surface area, and total pore volume of the sol-gel samples synthesized in the present work are summarized in Table 1 and compared with the data reported in the literature for Degussa P25 [15].

For the R100 sample, the TEM-DF image shows elongated particles distributed as daisy petals (Figure 4) with an average diameter 12.7 nm large and 26.0 nm long. The presence of a petal shape is confirmed by the HR-TEM micrographs, where they are shown grouped and isolated (Figure 5), with set of fringes corresponding to (110) lattice planes of rutile phase. The HR-TEM image of the R70 sample shows the features of the rutile phase and, in addition, the presence of square particles with average particle size of about 7 nm (Figure 6), with set of fringes not present in the R100 sample images and thus attributed to the presence of the anatase phase. The HR-TEM image of the mixed-phase R70 sample shows that the rutile and the anatase phases are in intimate contact.

3.2. EPR characterization of the catalysts

The EPR spectra of R100 and R70 samples were recorded at 10 K in helium atmosphere after 30 minutes of *in situ* UV irradiation (see Section 2). As a comparison, also the spectrum of Degussa P25 was recorded under the same conditions. For each sample, the absence of EPR signals on samples before irradiation was checked.

Spectra recorded on both R100 and R70 samples (Figure 7 (a) and (b), resp.) show the presence of a low-field signal attributable to holes trapped at O^{2-} species resulting in O^- centers ($g_\perp = 2.017$ and $g_{//} = 2.005$) [22] and of a poorly resolved axial signal attributable to trapped electrons at Ti^{3+} sites on rutile lattice ($g_\perp \sim 1.95$ and $g_{//} \sim 1.94$) [20]. Both these signals are observable also for the commercial product (Figure 7), even if this later shows more resolved resonance lines; however, the intensity of the signal attributable to the O^- species was higher for sol-gel samples than for Degussa P25, being 5 times higher for R100 and 3 times higher for R70 sample. Instead, the intensity of the Ti^{3+} signal is only slightly higher for sol-gel samples than for Degussa P25; this is in agreement with the results obtained by Berger et al. [22] that the relative ratio of Ti^{3+} and O^- signal intensities varies from sample to sample and that the Ti^{3+} concentration is always smaller (< 10%) than the concentration of trapped holes. The high amount of O^- centers detected on the sol-gel samples suggests that the UV irradiation induces an enhanced charge separation in these samples, with respect to Degussa P25, and/or that the charge carrier recombination rate is slower.

Table 1: XRD and N_2 adsorption-desorption results for the pure rutile (R100) and mixed-phase (R70) TiO_2, synthesized in the present study, compared with Degussa P25.

Sample	Phase content	Specific surface area (m^2/g)	Total pore volume (cm^3/g)
R100	rutile 100%	31	0.15
R70	anatase 30% + rutile 70%	44	0.23
Degussa P25	anatase 80% + rutile 20%	51	0.15

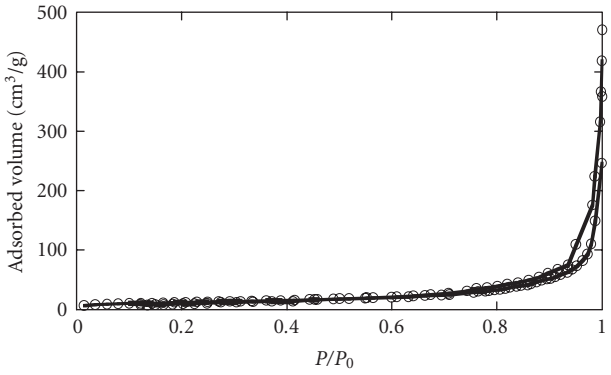

Figure 3: N_2-physisorption curves recorded at 77 K for the R70 TiO_2 catalyst.

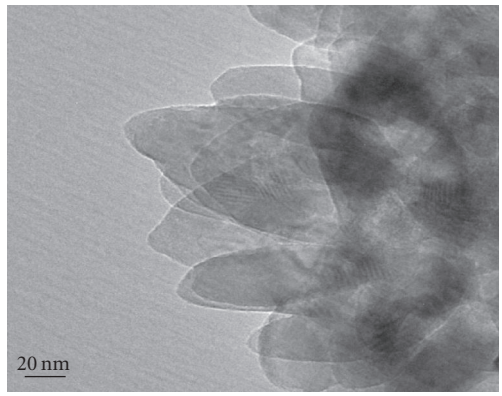

Figure 5: High-resolution transmission electron micrograph of the R100 TiO_2 catalyst.

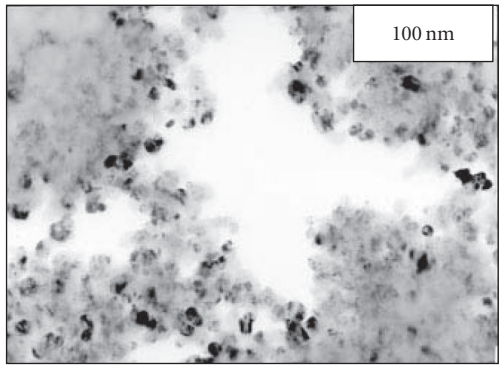

Figure 4: Trasmission electron microgaph of the R100 TiO_2 catalyst.

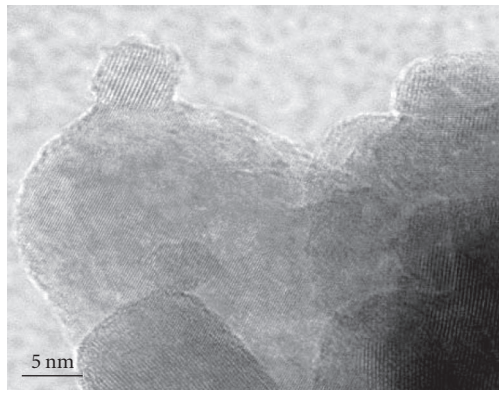

Figure 6: High-resolution transmission electron micrograph of the R70 TiO_2 catalyst.

On the other hand, the spectrum of the commercial product shows also the perpendicular components of the g-tensors attributable to trapped electrons at Ti^{3+} on anatase ($g_\perp = 1.989$) [20] and at the interface between anatase and rutile ($g_\perp = 1.980$) [19], these signals suggesting an electron transfer from rutile to anatase. In the case of sol-gel samples, these signals were not observed, this result suggesting that the stabilization of the charge separation in the sol-gel samples follows different ways than the rutile to anatase transfer.

3.3. Photoinduced degradation of phenol

Figure 8 shows the results of the photoinduced degradation of phenol in aqueous solution, catalyzed by R100 and R70, in terms of concentration of total organic carbon (TOC) at different reaction times (for experimental details, see Section 2). The initial concentration of phenol was 121 ppm, corresponding to 93 ppm of C (Figure 8). As a comparison, reactions were also carried out without TiO_2 (blank sample) and with Degussa P25. The maximum slope point, which corresponds to the maximum degradation speed, $(dC/dt)_{max}$, and the correspondent time value, $t_{1/2}$, are reported in Table 2. The results show a high activity for the R100 sample, which shows $(dC/dt)_{max} = 2.34$ ppm/min and $t_{1/2} = 29.9$ min, values slightly smaller than the commercial product ($(dC/dt)_{max} = 2.51$ ppm/min and $t_{1/2} = 27.5$ min). The R100 sample is much more active than R70 ($(dC/dt)_{max} = 2.03$ ppm/min and $t_{1/2} = 37.7$ min), which in turn is only slightly more reactive than

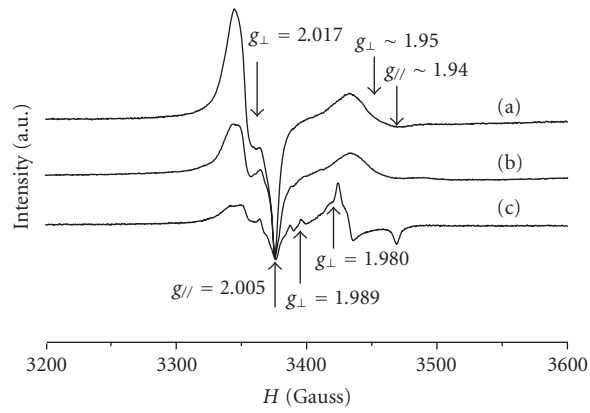

Figure 7: EPR spectra recorded at 10 K of (a) R100, (b) R70 TiO_2 sol-gel catalysts, and (c) commercial Degussa P25 after 30 minutes of *in situ* UV irradiation in helium atmosphere.

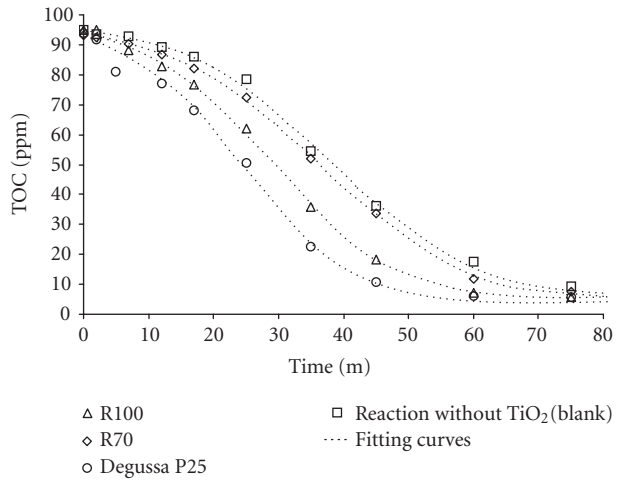

Figure 8: Photoinduced degradation of phenol with stoichiometric H_2O_2, catalysed by the following TiO_2 catalysts: (Δ) R100, (◊) R70, (O) Degussa P25. The symbol (□) indicates that the reaction was carried out without TiO_2 (blank). Dotted lines represent the fitting curves.

blank sample. These results agree with the amount of O^- centers, detected by EPR.

4. CONCLUSIONS

Nanocrystalline TiO_2 catalysts containing pure rutile (R100) and a mixed-phase 30% of anatase and 70% of rutile (R70) were synthesized by the sol-gel method, using the triblock copolymer Pluronic PE 6400 as templating agent.

With respect to the commercial product Degussa P25 [15], the two sol-gel catalysts show slightly lower BET surface area values, a low porosity and a much wider pore size distribution, with pore sizes ranging from 2 to 100 nm. This behavior is probably due to the prolonged calcination at 653 K, which was necessary in order to remove the triblock copolymer and obtain a white TiO_2 powder.

Table 2: Maximum degradation speed, $(dC/dt)_{max}$, and semitransformation time, $t_{1/2}$, calculated from the fitted curves reported in Figure 8.

Sample	$(dC/dt)_{max}$ (ppm/min)	$t_{1/2}$ (min)
Degussa P25	2.51	27.5
R100	2.34	29.9
R70	2.03	37.7
Blank	2.02	39.3

The EPR spectra recorded at 10 K under UV irradiation show that on the sol-gel samples electrons are trapped in Ti^{3+} sites on rutile phase and are not transferred to anatase. Moreover, the intensity of the signal attributable to the O^- species, resulting from the trapping of holes at bulk or surface anions, was higher for sol-gel samples than for Degussa P25, being 5 times higher for R100 and 3 times higher for R70 sample. This result suggests that the UV irradiation induces an enhanced charge separation in the sol-gel samples, with respect to the commercial product.

For what concerns the activity of these materials as catalysts in the degradation of phenol, the maximum degradation speed, $(dC/dt)_{max}$, and the semi-transformation time, $t_{1/2}$, calculated from the fitted curves, show that the R100 sample is only slightly less active than Degussa P25. Instead the R70 sample showed to be only slightly more reactive than blank sample, these results being in agreement with the relative amount of O^- centers detected by EPR.

The results obtained for the sol-gel samples in terms of porosity, amount of paramagnetic species and reactivity show that the wide pore distribution and the low porosity do not hinder to obtain a good reactivity in the degradation of phenol, this being in agreement with the enhanced charge separation observed by EPR. The stabilization of the charge separation in the sol-gel samples is probably due to different effects than those suggested for Degussa P25 [19–21]. On these bases, it is reasonable to expect that for R100 and R70 samples a higher reactivity can be obtained by increasing porosity.

REFERENCES

[1] D. M. Blake, P.-C. Maness, Z. Huang, E. J. Wolfrum, J. Huang, and W. A. Jacoby, "Application of the photocatalytic chemistry of titanium dioxide to disinfection and the killing of cancer cells," *Separation and Purification Methods*, vol. 28, no. 1, pp. 1–50, 1999.

[2] I. K. Konstantinou and T. A. Albanis, "Photocatalytic transformation of pesticides in aqueous titanium dioxide suspensions using artificial and solar light: intermediates and degradation pathways," *Applied Catalysis B: Environmental*, vol. 42, no. 4, pp. 319–335, 2003.

[3] K. Pirkanniemi and M. Sillanpää, "Heterogeneous water phase catalysis as an environmental application: a review," *Chemosphere*, vol. 48, no. 10, pp. 1047–1060, 2002.

[4] A. Heller, "Chemistry and applications of photocatalytic oxidation of thin organic films," *Accounts of Chemical Research*, vol. 28, no. 12, pp. 503–508, 1995.

[5] R. Cai, K. Hashimoto, K. Itoh, Y. Kubota, and A. Fujishima, "Photokilling of malignant cells with ultrafine TiO_2 powder," *Bulletin of the Chemical Society of Japan*, vol. 64, no. 4, pp. 1268–1273, 1991.

[6] X. Fu, W. A. Zeltner, M. A. Anderson, et al., "Applications in photocatalytic purification of air," in *Semiconductor Nanoclusters-Physical, Chemical, and Catalytic Aspects*, vol. 103 of *Studies in Surface Science and Catalysis*, pp. 445–461, Elsevier Science, Amsterdam, The Netherlands, 1997.

[7] P. Pichat, J. Disdier, C. Hoang-Van, D. Mas, G. Goutailler, and C. Gaysse, "Purification/deodorization of indoor air and gaseous effluents by TiO_2 photocatalysis," *Catalysis Today*, vol. 63, no. 2–4, pp. 363–369, 2000.

[8] T. Tatsuma, S. Saitoh, Y. Ohko, and A. Fujishima, "TiO_2-WO_3 photoelectrochemical anticorrosion system with an energy storage ability," *Chemistry of Materials*, vol. 13, no. 9, pp. 2838–2842, 2001.

[9] A. Mills, A. Lepre, N. Elliott, S. Bhopal, I. P. Parkin, and S. A. O'Neill, "Characterisation of the photocatalyst Pilkington Activ^{TM}: a reference film photocatalyst?" *Journal of Photochemistry and Photobiology A: Chemistry*, vol. 160, no. 3, pp. 213–224, 2003.

[10] L. Cassar, "Photocatalysis of cementitious materials: clean buildings and clean air," *MRS Bulletin*, vol. 29, no. 5, pp. 328–331, 2004.

[11] E. J. Wolfrum, J. Huang, D. M. Blake, et al., "Photocatalytic oxidation of bacteria, bacterial and fungal spores, and model biofilm components to carbon dioxide on titanium dioxide-coated surfaces," *Environmental Science and Technology*, vol. 36, no. 15, pp. 3412–3419, 2002.

[12] U. Stafford, K. A. Gray, P. V. Kamat, and V. Arvind, "An in situ diffuse reflectance FTIR investigation of photocatalytic degradation of 4-chlorophenol on a TiO_2 powder surface," *Chemical Physics Letters*, vol. 205, no. 1, pp. 55–61, 1993.

[13] G. Riegel and J. R. Bolton, "Photocatalytic efficiency variability in TiO_2 particles," *The Journal of Physical Chemistry*, vol. 99, no. 12, pp. 4215–4224, 1995.

[14] R. R. Bacsa and J. Kiwi, "Effect of rutile phase on the photocatalytic properties of nanocrystalline titania during the degradation of *p*-coumaric acid," *Applied Catalysis B: Environmental*, vol. 16, no. 1, pp. 19–29, 1998.

[15] G. Colón, M. C. Hidalgo, and J. A. Navío, "Photocatalytic deactivation of commercial TiO_2 samples during simultaneous photoreduction of Cr(VI) and photooxidation of salicylic acid," *Journal of Photochemistry and Photobiology A: Chemistry*, vol. 138, no. 1, pp. 79–85, 2001.

[16] R. F. Howe and M. J. Gratzel, "EPR observation of trapped electrons in colloidal titanium dioxide," *The Journal of Physical Chemistry*, vol. 89, no. 21, pp. 4495–4499, 1985.

[17] R. F. Howe and M. J. Gratzel, "EPR study of hydrated anatase under UV irradiation," *The Journal of Physical Chemistry*, vol. 91, no. 14, pp. 3906–3909, 1987.

[18] J. M. Coronado, A. J. Maira, J. C. Conesa, K. L. Yeung, V. Augugliaro, and J. Soria, "EPR study of the surface characteristics of nanostructured TiO_2 under UV irradiation," *Langmuir*, vol. 17, no. 17, pp. 5368–5374, 2001.

[19] D. C. Hurum, A. G. Agrios, S. E. Crist, K. A. Gray, T. Rajh, and M. C. Thurnauer, "Probing reaction mechanisms in mixed phase TiO_2 by EPR," *Journal of Electron Spectroscopy and Related Phenomena*, vol. 150, no. 2-3, pp. 155–163, 2006.

[20] D. C. Hurum, A. G. Agrios, K. A. Gray, T. Rajh, and M. C. Thurnauer, "Explaining the enhanced photocatalytic activity of Degussa P25 mixed-phase TiO_2 using EPR," *Journal of Physical Chemistry B*, vol. 107, no. 19, pp. 4545–4549, 2003.

[21] D. C. Hurum, K. A. Gray, T. Rajh, and M. C. Thurnauer, "Recombination pathways in the degussa P25 formulation of TiO_2: surface versus lattice mechanisms," *Journal of Physical Chemistry B*, vol. 109, no. 2, pp. 977–980, 2005.

[22] T. Berger, M. Sterrer, O. Diwald, et al., "Light-induced charge separation in anatase TiO_2 particles," *Journal of Physical Chemistry B*, vol. 109, no. 13, pp. 6061–6068, 2005.

[23] A. L. Attwood, D. M. Murphy, J. L. Edwards, T. A. Egerton, and R. W. Harrison, "An EPR study of thermally and photochemically generated oxygen radicals on hydrated and dehydrated titania surfaces," *Research on Chemical Intermediates*, vol. 29, no. 5, pp. 449–465, 2003.

[24] P. Yang, D. Zhao, D. I. Margolese, B. F. Chmelka, and G. D. Stucky, "Generalized syntheses of large-pore mesoporous metal oxides with semicrystalline frameworks," *Nature*, vol. 396, no. 6707, pp. 152–155, 1998.

[25] H. Luo, C. Wang, and Y. Yan, "Synthesis of mesostructured titania with controlled crystalline framework," *Chemistry of Materials*, vol. 15, no. 20, pp. 3841–3846, 2003.

[26] S. Brunauer, P. H. Emmett, and E. Teller, "Adsorption of gases in multimolecular layers," *Journal of the American Chemical Society*, vol. 60, no. 2, pp. 309–319, 1938.

Special Issue on
Lasers in the Preservation of Cultural Heritage

Call for Papers

During the Laser Optics Conference held in St. Petersburg, Russia, a workshop on Lasers in the Preservation of Cultural Heritage was organized.

A special issue based on this workshop aims to focus on the following topics:

- Needs and approaches in conservation: what are the needs, approaches, and limitations?
- Documentation and diagnostics:
  - Analysis of composition
  - Structural diagnostics by NDT
- Laser interventions: cleaning and restorations
- Case studies

Authors should follow the LC manuscript format described at http://www.hindawi.com/GetJournal.aspx?journal=LC. Prospective authors should submit an electronic copy of their complete manuscript through the LC manuscript tracking system at http://www.hindawi.com/mts/, according to the following timetable:

Manuscript Due	September 15, 2006
Acceptance Notification	October 31, 2006
Final Manuscript Due	November 30, 2006
Publication Date	4th Quarter, 2006

GUEST EDITORS:

Costas Fotakis, Institute of Electronic Structure and Laser (IESL), Foundation for Research and Technology - Hellas (FORTH), P.O. Box 1385, Vassilika Vouton, 71110 Heraklion, Crete, Greece; fotakis@iesl.forth.gr

Wolfgang Kautek, Institut of Physical Chemistry, University of Vienna, 1010 Vienna, Austria;
wolfgang.kautek@univie.ac.at

Marta Castillejo, Spanish National Research Council (CSIC), Serrano 117, 28006 Madrid, Spain;
marta.castillejo@iqfr.csic.es

Special Issue on
Advances in Optical Nanomaterials

Call for Papers

The special issue Advances in Optical Nanomaterials aims to collect recent research results on the concepts, formation and (potential) application of nanostructured materials suitable as active or passive optical elements. In this context, the term optical is not limited to the visible range of the spectrum, but extends to the ultraviolet as well as to near and far infrared and even to THz radiation. Applications may cover optical coatings for sensors or solar cells, diffractive elements or films for novel optics or imaging, new materials for optical data storage, photonic crystals and metamaterials having a negative index of refraction or nanostructures suitable as emitters or detectors of radiation down to the THz-regime. Apart from materials research, device concepts as well as manufacturing aspects are welcome.

Intended for both industry and academia, and by providing speedy turnaround review and thus quick publication of original short and lengthy articles, followed by free-access, AOE aims to accelerate worldwide recognition, dissemination and utilization of the most recent findings and advances in optoelectronics.

Authors should follow the AOE manuscript format described at http://www.hindawi.com/GetJournal.aspx?journal=AOE. Prospective authors should submit an electronic copy of their complete manuscript through the AOE Manuscript Tracking System at http://www.hindawi.com/mts/, according to the following timetable:

Manuscript Due	November 15, 2006
Acceptance Notification	January 1, 2007
Final Manuscript Due	February 15, 2007
Publication Date	2nd Quarter, 2007

GUEST EDITOR:

Ralf Bergmann, ROBERT BOSCH GMBH, Zentralabteilung Forschung und Vorausentwicklung, Abteilungsleiter, Abteilung Angewandte Physik (CR/ARP), Postfach 10 60 50, D-70049 Stuttgart, Germany;
ralf.bergmann@de.bosch.com